Rectal tumor boundary detection by unifying active contour model

Di Xiao[a], Wan Sing Ng[a], Udantha R. Abeyratne[b], Charles Bih-Shiou Tsang[c]
[a]School of Mechanical & Production Eng., [b]School of Electrical & Electronic Eng., Nanyang Technological Univ.; [c]Dept. of Colorectal Surgery, Singapore General Hospital, Singapore

ABSTRACT

The Project of 3D reconstruction of rectal wall structure aims at developing an analysis system to help surgeons cope with a large quantities of rectal ultrasound images, involving muscular layer detection, rectal tumor detection, and 3D reconstruction, etc. In the procedure of tumor detection, a traditional active contour model suffers some difficulties for finding the boundary of tumor when it deforms from the "seed" in the interior of a tumor. In this paper, we proposed a novel united active contour model with the information of image region feature and image gradient feature for the purpose of tumor detection. Region-based method added in the model, however, introduces a statistical method into the segmentation of the image and hence becomes less sensitive to noise. The originality in this algorithm is that we introduce a Gaussian Mixture Model (GMM) into the statistical model description of "seed" region. This model can perform more accurate and optimal statistical description than a single Gaussian model. A K-means algorithm and an Expectation Maximization (EM) algorithm are used for optimal parameter estimation of GMM. The experimental results show the new model has more optimal performance for image segmentation and boundary finding than classical active contour model.

Keywords: Active contour model, Rectal wall ultrasound image, Gaussian Mixture Model, Expectation Maximization

1. INTRODUCDTIONS

Endoscopic ultrasonography (EUS) has become one of the most common techniques for screening test and early staging of the colorectal tumors. One of the advantages of EUS is that it can get cross-sectional images of the rectum[3, 4]. From these cross-sectional images, the anatomical structure of the organs and the situation of tumors are clearly displayed. The goal of our project is to develop an automatic or semi-automatic analysis system to aid surgeons to cope with large quantities of rectal ultrasound images, involved rectal layer detection, rectal wall tumor detection, 3D reconstruction of rectal anatomic structure and corresponding quantitative analysis. This will be greatly helpful for the early stage diagnosis of rectal cancer. In this paper, we focus on the boundary detection algorithm for tumor.

Rectal tumor is a special region with different gray level features from balloon region and muscular layers in a rectal ultrasound image. The big difficulty for rectal tumor boundary detection is the non-homogeneity feature of the tumor region. Therefore, low-level image processing method is not suitable for its boundary detection. The high-level boundary detection algorithm like active contour we used for rectal muscular layer detection also suffer from this difficulty because the boundary information in the algorithm is only dependent on the gradient feature of image. From a more extensive point of view, rectal tumor boundary detection is not just a boundary detection issue but an issue of region segmentation. In this paper, we are keen on how to enhance the function of active contour algorithm that we are familiar with and integrate some basic principle of region segmentation with it to implement tumor boundary detection. In the following, we will give a brief review of image segmentation and the combination of region segmentation and boundary finding.

The segmentation of a given image is one of the important techniques for image analysis, understanding. It is one of basic approaches in the area of image processing. Most segmentation methods can be divided into two basic image processing techniques: boundary-based segmentation method and region-based segmentation method. One kind of boundary-based method is based on contour deformation like snakes, point distribution model, level set and graph searching methods. They usually use a closed curve to approximate the desired object under the guide of the image features and hard constraints from the priori knowledge. But they may have the problems of stability and convergence, such as arriving at a local minimum. The region-based segmentation methods are more suitable for the area segmentation on the image. The statistical algorithm is a core tool used by this method. Two kinds of famous approaches are region-growing method and Markov Random Field methods.

Medical Imaging 2002: Image Processing, Milan Sonka, J. Michael Fitzpatrick,
Editors, Proceedings of SPIE Vol. 4684 (2002) © 2002 SPIE · 1605-7422/02/$15.00

A series of efforts have been done recently to integrated boundary and region information in one model for image segmentation. Haddon [1] proposed a two-stage segmentation method. In the first stage, an initial pixel classification is obtained by analyzing the distribution of the co-occurrence matrices. Then, a region information for each region is estimated from its corresponding co-occurrence matrix and expressed by conditional probabilities (as a priori). In the second stage, the local consistency of pixel classification is implemented and updated by minimizing the entropy of local region information. Pavlidies [2][3] proposed a method that unifies the traditional region growing and edge detection methods for image segmentation. The first step is to obtain a whole segmentation results by splitting and merging approaches. In the following step, based on the above results, a border finding algorithm is used to eliminate and modify the boundaries and finally find the segmentation regions. The similar work was also done by Jianhua Xuan for brain MRI image segmentation [4]. They all use edge information to correct the segmentation result obtained by region growing algorithm.

T. F. Chan [5][6] proposed an active contour model without edges, which is based on the techniques of curve evolution, Mumford-Shah functional for segmentation, and level set method. The new idea different from the classical snakes is that the stopping rule is not dependent on the gradient term from the image, but instead is based on Mumford-shah segmentation method. This stopping term is actually a function that realize the comparison of two image intensity terms inside the evolving curve and outside the curve with the average intensity terms inside and outside the curve, respectively. The main limitation of the model is that some objects can not be detected only using the intensity information. C. Z. Song [7] proposed a statistical framework for multi-band image segmentation called region competition, which unifies snakes, region growing, and Bayes/Minium Description Length (MDL) method. This algorithm is derived from the Bayes and MDL for image segmentation using global energy function criteria. The implementation of the algorithm is actually a combination of classic snake algorithm and statistical techniques of region growing. This work has some similarities to the works [8][9]. They all use the statistical approaches to find the seed regions in the image, and then use the MDL criteria to compress the overlapping between regions. Although a snake/balloon model is used for segmentation process, it is only used to constrain the regularity of the curve that seems ignoring the border information from image.

The problem in [7] pointed out in [10] is the final solution lacks the notion of shape because the integration is primarily carried out in a local pixel-wise sense. In the method proposed by Charkraborty [10], the author solves the boundary estimation problem by using gradient and region homogeneity information in the maximum *a posteriori* framework. Then, Green's theorem is used to derive the boundary of a homogenous region and an image gradient-based boundary finder is incorporated into it. The author emphasized that the difference of this method is to integrate the boundary finding rather than edge detection into the region-based segmentation. The main problem with this approach is the region information is denoted by intensity homogeneity, therefore it limits the applicability of the model. And the contour model is set up by Fourier descriptors, which also limits the description of the object's shape.

Recently, Nikos Paragios introduced the region-based segmentation algorithm into the geodesic active contour algorithm and obtained a unifying boundary and region-based model called Geodesic Active Region [11]. The defined objective function is minimized by a gradient-descent algorithm. The contour is propagated towards the object boundary guided by boundary forces, region forces and external forces. A level set method is help to implement the corresponding partial differential equation (PDE) of the objective function. This model was applied for several image processing areas, such as image segmentation [12], boundary finding and motion tracking [13]. The similar approach is also applied in the segmentation of the left ventricle from MR cardiac images.

2. A UNIFYING ACTIVE CONTOUR MODEL

For image segmentation, different regions have their own distinct features. One of the methods to describe these features is by statistical models. In the region-based segmentation algorithm, especially "seed" algorithm, the statistical properties of the seed region is particularly important for deciding the growing of the seed region. The neighboring pixels will be classified into the seed region or not by comparing the similarity of the statistical features between them and seed region.

The active contour model (snakes) proposed is only based on the gradient features (boundary information). In this section, we will pay more attention on the efficacy of region information. We aim at proposing a unifying region- and boundary-based active contour model. The region information is from the conditional probability distribution for that specific region. We focus on seeking a more accurate statistical characteristic description for seed region. Therefore, we propose that a region's statistical features should be described accurately by a Gaussian Mixture Model (GMM).

Expectation-Maximization (EM) algorithm is used to compute the parameters in GMM. This novel model can be used for general purpose of image segmentation. In particularly, it is aimed to solve the tumor boundary finding in our project.

2.1 Framework of the unifying active contour model

A novel model is set up based on the framework of Mumford-shah model, and defined as

$$E(U,K) = \iint_{\Omega\setminus K} (|\nabla U(x,y)|^2\, dxdy + \iint (U(x,y) - I(x,y))^2) dxdy + length(K). \tag{1}$$

Therefore, the energy that describes the segmentation of the image consists of three main energies: boundary-based energy, region-based energy and contour constraint energy.

2.1.1 Boundary-based energy module

This module that decides the boundary finding of the object is based on the boundary information. Here we choose the gradient magnitude from the image as the boundary information of the object like traditional approach. The energy module corresponds to setting

$$E_{img}(\partial R) = \iint |\nabla I(x,y)| dxdy \tag{2}$$

Thus, the segmentation of image or object detection is to find the boundary that has the maximum energy on the gradient magnitude field of the image.

2.1.2 Region-based energy module

For general, the region-based energy module aims at classifying an image into a number of regions by region information. The object boundary finding, while an object placed on a background can be considered a special case of image segmentation, which segments object from its background image. Assume that the object data set is denoted by $\mathbf{I}_O$ and background data set $\mathbf{I}_B$. The image segmentation task is to create a consistent frame partition between the observed data set, the associated judging criteria. Here, we use the maximum *a posteriori* method as the classification criteria. Thus, the segmentation problem becomes the optimization problem of *a posteriori* probability. With a given intensity image, the maximum *a posterior* distribution of the regions can be expressed by maximizing $p(R(\mathbf{I})\,|\,\mathbf{I})$, which means with given image $\mathbf{I}$ make the probability of different regions $R(\mathbf{I})$ maximization. The density probability function is

$$p(R(\mathbf{I})\,|\,\mathbf{I}) = p(\{R(\mathbf{I}_O), R(\mathbf{I}_B)\}\,|\,\mathbf{I}) \tag{3}$$

Where, $R(\mathbf{I}_O) = \{I_{(x,y)} : (x,y) \in \mathbf{I}_O\}$ represents the intensity of each pixel that belongs to the object region and $R(\mathbf{I}_B) = \{I_{(x,y)} : (x,y) \in \mathbf{I}_B\}$ intensity of each pixel that belongs to the background region. Based on the Bayes rule, we can deduce that maximizing *a posteriori* probability is equal to maximizing following equation, when assuming the sample of the image pixel is independent each other,

$$p(R(\mathbf{I})\,|\,\mathbf{I}) = p(\mathbf{I}\,|\,R(\mathbf{I}_O))\,p(\mathbf{I}\,|\,R(\mathbf{I}_B)) = \prod_{(x,y)\in R(\mathbf{I}_O)} p_O(I(x,y)) \prod_{(x,y)\in R(\mathbf{I}_B)} p_B(I(x,y)) \tag{4}$$

As a result, the issue of maximizing a posteriori probability for a region $R(\mathbf{I})$ with respect to a given image becomes that of maximizing the product of each region's probability.

Usually, we take $-\log()$ on the above formula and change the solution of maximizing of the probability distribution into that of minimizing the $-\log()$ function of the energy, in order to be consistent with other energy terms. It is reasonable, for $-\log()$ is a monotonic decrease function. Thus the region-based energy can be defined as

$$E_{regn}(\partial R(\mathbf{I})) = -\log\left(\prod_{(x,y)\in R(\mathbf{I}_O)} p_O(I(x,y)) \prod_{(x,y)\in R(\mathbf{I}_B)} p_B(I(x,y))\right) \tag{5}$$
$$= -\iint_{(x,y)\in R(\mathbf{I}_O)} \log\big(p_O(I(x,y))\big)dxdy - \iint_{(x,y)\in R(\mathbf{I}_B)} \log\big(p_B(I(x,y))\big)dxdy$$

From above formulation, we know that when a pixel is classified correctly, such as belonging to object area, the probability $p_O(I(x,y))$ will be greater than $p_B(I(x,y))$, otherwise, the probability $p_B(I(x,y))$ greater than $p_O(I(x,y))$.

So, in summary, the region-based energy is defined to maximize the *a posterior* probability of the region information. For multiple regions' segmentation, multiple seeds are needed to place on their respective regions. The splitting and merging techniques can be applied during the segmentation process. Therefore, multiple probability distributions are required to set up for describing different regions. For the special case such as boundary finding of a single object, one initial contour seed with its corresponding probability distribution and background's is needed for region description.

2.1.3 Contour internal energy module

For the constraint of the contour's feature, we borrow the concept from snakes that the tension and rigidity of the contour is constrained by its first- and second- derivatives. The energy term is denoted by

$$E_{\text{int}}(\partial C) = \iint ((\partial(s)|v_s(s)|^2 + \beta(s)|v_{ss}(s)|^2)/2)ds \tag{6}$$

where, $v(s)$ is the node on the contour expressed by arc length s, $v_s(s)$ and $v_{ss}(s)$ are first- and second-derivatives with respect to arc length, respectively, and $\partial(s)$ as well as $\beta(s)$ are corresponding weights.

2.1.4 Energy module and its kinetic function

To combine above three energy modules, we obtain our active contour model as follows

$$E(\partial C) = w_{regn}\left[-\iint_{(x,y)\in R(\mathbf{I}_O)} \log\big(p_O(I(x,y))\big)dxdy - \iint_{(x,y)\in R(\mathbf{I}_B)} \log\big(p_B(I(x,y))\big)dxdy\right] + \tag{7}$$
$$w_{grad}\left[\iint |\nabla I(x,y)|dxdy\right] + \iint ((\partial(s)|v_s(s)|^2 + \beta(s)|v_{ss}(s)|^2)/2)ds$$

where, w_{grad}, w_{reg} are weight parameters.

In order to deform the active contour, we should derive its the numerical solution. We have known that the minimum of the energy function is the stable solution of the contour. Above defined objective function can be minimized using a gradient descent method. Through Euler-Lagrange algorithm, we can obtain the kinetic function of the active contour as

$$\frac{\partial}{\partial t}\partial(C) = w_{grad}\nabla|\nabla I(x,y) \bullet \nabla I(x,y)| - w_{regn}\log\left(\frac{p_O(I(x,y))}{p_B(I(x,y))}\right)\vec{\mathrm{n}}_O(\partial C) \tag{8}$$
$$+ \alpha(s)v_{ss}(s) + \beta(s)v_{ssss}(s)$$

Three forces decide the motion of a contour point. They are internal force, region force, and boundary force (or gradient force). Fig. 1 illustrates the function of these three forces respectively.

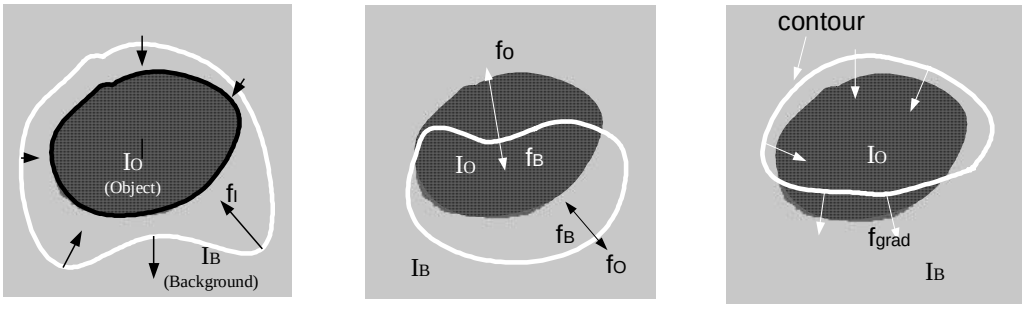

(a) Internal forces (b) Region forces (c) Boundary forces.

Fig. 1: Three kinds of forces: Internal forces (f_I), region force (f_O, f_B) and gradient forces (f_{grad})

2.2 Gaussian mixture model (GMM) and EM algorithm

In this subsection, we will discuss how to set up an accurate statistical model for a specific image region by GMM algorithm and how to get the optimal parameters solution for setting up this GMM. First, we will give a brief introduction of EM algorithm. Then we will introduce it into the parameter solution of GMM.

2.2.1 EM algorithm

The EM algorithm is a broadly applicable method that uses an iterative procedure to find the maximum-likelihood estimate of the parameters from an observed data set when these data are considered as incomplete data. In general, the maximization of the likelihood function $l(\Theta \mid \mathbf{I})$ (where, I is observed data, and Θ is the parameters) is very complicated and may have no analytic solution. But by introduce the data set some intermediate variables, also called "latent data" or missing data ($\mathbf{Y} = \{Y_1, Y_2, ..., Y_i\}$), which are never observable, it has shown that the estimation problems of maximum-likelihood becomes easily analytic solvable. For many statistical problems this complete-data likelihood estimation has a nice form.

EM algorithm can be described by following two steps. The first step is E (Expectation) step and the second step is M (Maximization) Step. E step is to find the expected value of the complete-date likelihood function,

$$Q(\Theta, \Theta^{(i-1)}) = E[\log p(\mathbf{I}, \mathbf{Y} \mid \Theta) \mid \mathbf{I}, \Theta^{(i-1)})] = \int \log p(\mathbf{Y}, \mathbf{I} \mid \Theta) p(\mathbf{Y} \mid \mathbf{I}, \Theta^{(i-1)}) d\mathbf{Y} \tag{9}$$

Please not that $p(\mathbf{Y} \mid \mathbf{I}, \Theta^{(i-1)})$ is the marginal density function of the latent data and is governed by the observed data and the current parameters $\Theta^{(i-1)}$.

The second step is M step, which is to maximize above expectation by iterative procedure and get the parameters Θ, as

$$\Theta^{(i)} = \arg\max_{\Theta} Q(\Theta, \Theta^{(i-1)}) \tag{10}$$

2.2.2 Gaussian Mixture Model

A multivariate Gaussian mixture model can be denoted by a weighted sum of single d-dimensional Gaussian component distribution,

$$p(\mathbf{I} \mid \Theta_i) = p(\mathbf{I} \mid \mu_i, \Sigma_i) = (2\pi)^{-d/2} \left| \Sigma_i \right|^{-1/2} \exp\left[-\frac{(\mathbf{I} - \mu_i) \Sigma_i^{-1} (\mathbf{I} - \mu_i)}{2} \right] \tag{11}$$

Where i expresses i-th component, μ_i is mean and Σ_i the covariance matrix, collectively expressed by the parameter vector Θ_i. A general form of GMM can be denoted as

$$\begin{cases} p(\mathbf{I} \mid \Theta) = \sum_{i=1}^{M} \alpha_i p(\mathrm{I_j} \mid \Theta_i) \\ \sum_{i=1}^{M} \alpha_i = 1 \end{cases} \tag{12}$$

For the purpose of our project, we set up a GMM comprising of three weighted Gaussian components, expressed by

$$p(\mathbf{I} \mid \Theta) = \alpha_1 p_1(\mathbf{I} \mid \mu_1, \Sigma_1) + \alpha_2 p_2(\mathbf{I} \mid \mu_2, \Sigma_2) + \alpha_3 p_3(\mathbf{I} \mid \mu_3, \Sigma_3) \tag{13}$$

The parameter solution of this Gaussian model becomes the estimation of the following nine parameters $\mathbf{\Phi} = \{\alpha_1, \alpha_2, \alpha_3, \mu_1, \mu_2, \mu_3, \sigma_1, \sigma_2, \sigma_3,\}$. As we have introduce above, the next task is to estimate the parameters $\{\alpha_i, \mu_i, \Sigma_i\}$ of each Gaussian component by maximizing the likelihood function,

$$l(\Phi \mid \mathbf{I}) = \sum_{j=1}^{N} \ln\left(\alpha_1 p_1(\mathrm{I_j} \mid \mu_1, \Sigma_1) + \alpha_2 p_2(\mathrm{I_j} \mid \mu_2, \Sigma_2) + \alpha_3 p_3(\mathrm{I_j} \mid \mu_3, \Sigma_3)\right) \tag{14}$$

In order to get the maximization of the likelihood function; we need to solve their corresponding partial differential equations with respect to the parameters μ_i, Σ_i as follows

$$\begin{aligned} \frac{\partial l(\Phi \mid \mathbf{I})}{\partial \mu_i} &= \sum_{j=1}^{N} \frac{1}{\alpha_1 p_1(\mathrm{I_j} \mid \mu_1, \Sigma_1) + \alpha_2 p_2(\mathrm{I_j} \mid \mu_2, \Sigma_2) + \alpha_3 p_3(\mathrm{I_j} \mid \mu_3, \Sigma_3)} \frac{\partial p_i(\mathrm{I_j} \mid \mu_i, \sigma_i)}{\partial \mu_i} \\ &= \sum_{j=1}^{N} \frac{\alpha_i p_i(\mathrm{I_j} \mid \mu_i, \sigma_i)}{\alpha_1 p_1(\mathrm{I_j} \mid \mu_1, \Sigma_1) + \alpha_2 p_2(\mathrm{I_j} \mid \mu_2, \Sigma_2) + \alpha_3 p_3(\mathrm{I_j} \mid \mu_3, \Sigma_3)} \left(\frac{\mathrm{I_j} - \mu_i}{{\sigma_i}^2}\right) \\ &= \sum_{j=1}^{N} p(i \mid \mathrm{I_j}) \left(\frac{\mathrm{I_j} - \mu_i}{{\sigma_i}^2}\right) = 0 \end{aligned} \tag{15}$$

$$\begin{aligned} \frac{\partial(\Phi \mid \mathbf{I})}{\partial \sigma_i} &= \sum_{j=1}^{N} \frac{1}{\alpha_1 p_1(\mathrm{I_j} \mid \mu_1, \Sigma_1) + \alpha_2 p_2(\mathrm{I_j} \mid \mu_2, \Sigma_2) + \alpha_3 p_3(\mathrm{I_j} \mid \mu_3, \Sigma_3)} \frac{\partial p_i(\mathrm{I_j} \mid \mu_i, \sigma_i)}{\partial \sigma_i} \\ &= \sum_{j=1}^{N} \frac{\alpha_i p_i(\mathrm{I_j} \mid \mu_i, \sigma_i)}{\alpha_1 p_1(\mathrm{I_j} \mid \mu_1, \Sigma_1) + \alpha_2 p_2(\mathrm{I_j} \mid \mu_2, \Sigma_2) + \alpha_3 p_3(\mathrm{I_j} \mid \mu_3, \Sigma_3)} \left(\frac{(\mathrm{I_j} - \mu_i)^T (\mathrm{I_j} - \mu_i)}{{\sigma_i}^3} - \frac{d}{\sigma_i}\right) \\ &= \sum_{j=1}^{N} p(i \mid \mathrm{I_j}) \left(\frac{(\mathrm{I_j} - \mu_i)^T (\mathrm{I_j} - \mu_i)}{{\sigma_i}^3} - \frac{d}{\sigma_i}\right) = 0 \end{aligned}$$

and get their final expressions as

$$\mu_i = \frac{\sum_{j=1}^{N} p(i \mid \mathrm{I_j}) \mathrm{I_j}}{\sum_{j=1}^{N} p(i \mid \mathrm{I_j})}, \quad \sigma_i = \frac{\sum_{j=1}^{N} p(i \mid \mathrm{I_j})(\mathrm{I_j} - \mu_i)^T (\mathrm{I_j} - \mu_i)}{d \sum_{j=1}^{N} p(i \mid \mathrm{I_j})}, \quad \alpha_i = \frac{1}{N} \sum_{j=1}^{N} p(i \mid \mathrm{I_j}), \quad i = 1,2,3 \tag{16}$$

In general, we can estimate the parameters (α_i, μ_i, σ_i) from themselves equations respectively. But because the posteriori probability included in three solution equations is still the function of the parameters (α_i, μ_i, σ_i), these three equations are actually to form a nonlinear system of three equations. It is hard to get the solution by general methods. Usually, the iterative method is introduced to solve this kind of problem. In a number of iterative methods, EM algorithm is a good method with many advantageous features than others.

In the following, we give the steps that use EM algorithm to get the optimal solution of the parameters,

1. Compute the initial values for the parameter $\Phi = [\alpha_i, \mu_i, \sigma_i]$ by K-means algorithm, where $i = 1, 2, 3$.
2. Calculate the *a posteriori* probability distributions $p(i \mid I_j)$ by using obtained Φ, where $i = 1, 2, 3$, and $j = 1, \ldots, N$.
3. For *a posteriori* probability distributions have known, the parameter $\Phi = [\alpha_i, \mu_i, \sigma_i]$ can be calculated directly by Eq. (16).
4. A new set of the estimate parameter $\Phi = [\alpha_i, \mu_i, \sigma_i]$ is obtained. If the sequence of Φ becomes steady, such as $\left\| \Phi - \hat{\Phi} \right\|$ is less than a threshold, the EM algorithm is ended, otherwise, we return to the step 2 for further calculation.

3. EXPERIMENTS AND DISCUSSION

3.1 Boundary finding on a synthetic image

We firstly use a synthetic image to test the new feature of this novel unifying active contour model. The image can be considered as a structure of multiple ring-shaped objects, which are similar concentric. The average gray value of all "white" regions is 192, and that of all "black" regions 128. The standard deviation of the noise is 68. It is very clear that the low-level thresholding method is not suitable for boundary detection because the standard deviation of the noise is greater than the difference of gray values between two regions.

As shown in Fig. 3 (a), the initial contour is placed in the interior of the center object region. Then the region's statistical information is computed from the pixels in the interior of the contour. In the computing progress, the K-means algorithm and EM algorithm help to complete the parameter estimation of the GMM which is composed of three weighted Gaussian functions to describe the pixels' gray level distribution. After obtaining the GMM, kinetic equation Eq. (8) is used to deform the active contour. At present, active contour deforms under the constraints of the internal forces, region forces and gradient forces. Fig. 3 (b) shows one result of the innermost boundary finding by unifying active contour model. The weighting parameters are listed in Table 1.

In the following, an experiment is designed to test the sensitivity of the weighting coefficient of region. As we have known from Eq. (8), the region force is represented by $\log\left(\frac{p_O(I(x,y))}{p_B(I(x,y))}\right)$. $p_O(I(x,y))$ is a GMM representing the statistical features of the seed region. We use its normalized value in our algorithm. The p.d.f. $p_B(I(x,y))$, which represents the statistical features of the background region, is not known. In the experiment, $p_B(I(x,y))$ is set to be a function related to the value of $p_O(I(x,y))$. When the $p_O(I(x,y))$ value is greater than 0.1, the $p_B(I(x,y))$ value is set to constant 0.1, otherwise, $p_B(I(x,y))$ value will gradually increase with the decrease of the corresponding $p_O(I(x,y))$ value, as shown in Fig. 2.

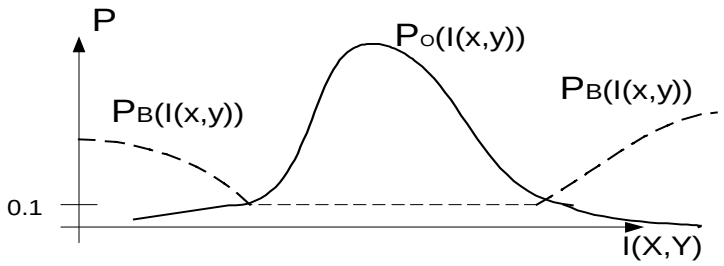

Fig. 2: Setting the background probability model

Table 1: Parameter setting of the united active contour for synthetic image

α	β	l	w_{grad}	w_{regn}
0.029	0	1	25	0.045

Because of the variability of the $p_B(I(x,y))$, the background statistical information is emphasized in $\log\left(\frac{p_O(I(x,y))}{p_B(I(x,y))}\right)$. Therefore, when a contour node goes into the background region, a greater background region force will create and push this contour node go back into the object region. With the enhancement of the effect of region force, the sensitivity of the weighting coefficient w_{regn} is reduced compared to only set $p_B(I(x,y))$ as a constant like 0.1. The variable scope of w_{regn} is enlarged to 0.034 –0.13. Fig. 3 (b) and (c) show the results for two different weighting coefficients in the stable scope. Fig. 3 (d) give a failure result when weighting value is chosen out of the stable scope. As we know, too large region weighting coefficient will reduce the effect of gradient force, and make the contour easily be attracted by some noise points and cause the contour run over the real boundary.

Table 2: Parameter setting for Tumor detection

α	β	l	w_{grad}	w_{regn}
0.029	0	1	58	0.05

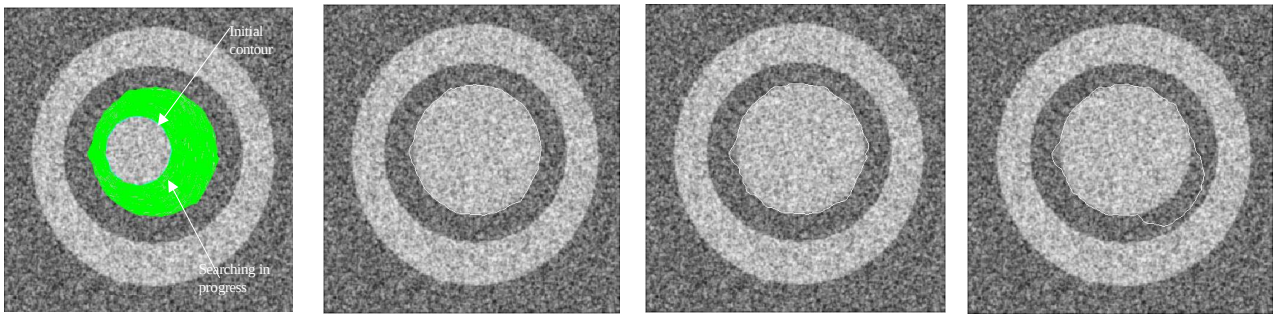

(a) Searching in progress (b) w_{regn} = 0.045 (c) w_{regn} = 0.12 (d) w_{regn} = 0.14

Fig. 3: The characteristics of region force weighting in the second experiment

3.2 Application and Assessment

3.2.1 Tumor boundary detection

In this subsection, we will demonstrate the performance of the unifying active contour model on some real data. The weighting coefficients are chosen as listed in Table 2. They are kept consistency with that in the previous experiment except the gradient weighting coefficient is set as a larger value. Fig. 5 illustrates a common procedure of tumor boundary finding. First, the initial contour is placed in the tumor region. Then, the interior of the contour is used as seed region to compute the regional statistical parameters and following that a GMM is constructed using these statistical parameters. The active contour starts to deform under the constraints of kinetic function based on the gradient force, region force and internal force. Fig. 4 (a) illustrates the histogram of gray level of the pixels in the initial contour region. Fig. 4 (b) gives the computed GMM computed from this histogram, which describe the statistical feature of the initial contour region. Fig. 5 (a) shows the progress of contour deformation and Fig. 5 (b) gives the final detected result of the tumor boundary. Fig. 6 shows the results of tumor boundary finding on other three rectal wall images.

It is obvious that the choice of the weighting coefficients will influence the balance between three forces and therefore effect the final experimental result. For example, if we want to emphasize the effect of the region force, we can increase its weighting coefficient. We can also decrease its weighting coefficient or increase the gradient weighting coefficient to strengthen the effect of the gradient force. Fig. 7 gives several experimental results for setting different regional weighting coefficients on the detection of the same tumor.

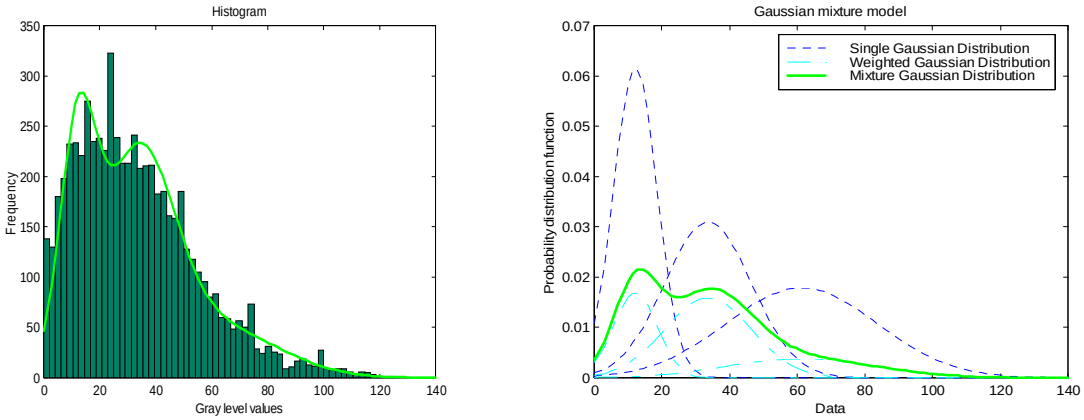

Fig. 4: Histogram of the pixel intensity of tumor region and Gaussian Mixture Distribution

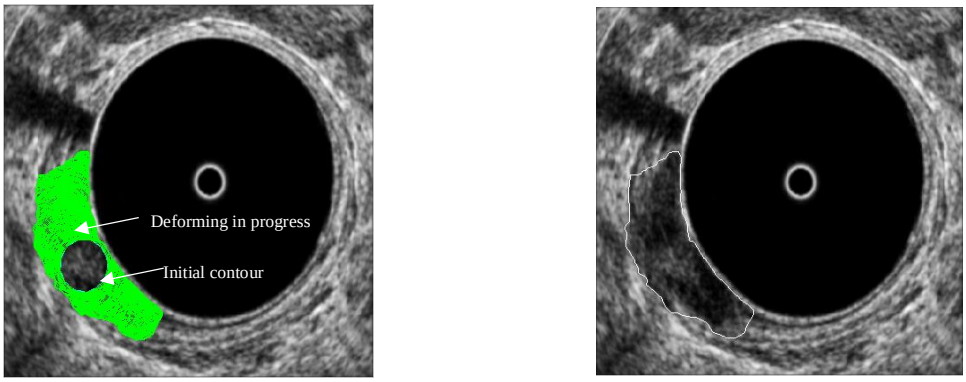

(a) Deformation in progress (Image no. 19991025_06)

(b)Tumor boundary

Fig. 5: Tumor boundary detection by unified active contour.

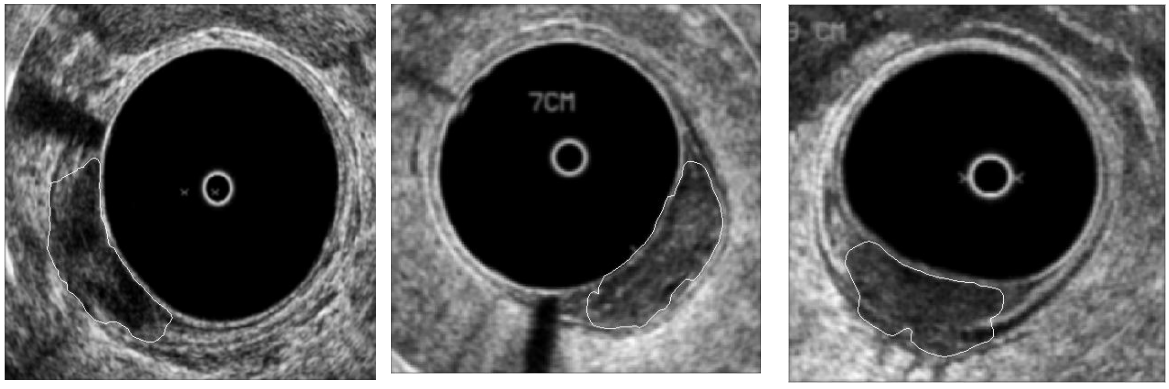

(a)Image no. 19991025_07

(b) Image no. 19991101_01

(c) Image no. 19991109_04

Fig. 6: A series of results of tumor boundary detection

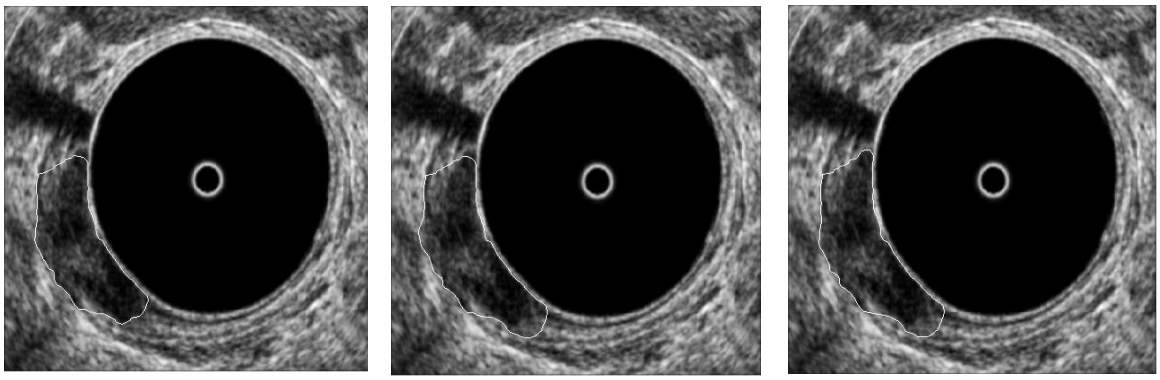

(a) w_{regn} =0.0350 (b) w_{regn} =0.0450 (c) w_{regn} =0.0600

Fig. 7: A comparison about the influence of the different region weighting coefficients to detecting results (Image no. 19991025_06)

3.2.2 Assessment of the results

A surgeon was invited to evaluate the results of boundary detection. The adopted method is to have experts to delineate the boundary of the tumor and compare this manual result with the automatic result by our algorithm. We use the statistical method to compare the automatic result with the manual delineation. Suppose S_a is the area of the obtained contour, and S_m the area of the delineated contour. We compare the similarity by following two formulae, which compute the relative values of the two areas' agreement,

$$l_{AND} = \frac{AND(S_a, S_m)}{OR(S_a, S_m)}, \qquad l_{XOR} = \frac{XOR(S_a, S_m)}{OR(S_a, S_m)} \tag{17}$$

where, l_{AND} and l_{XOR} are the ration of the common (AND operation) area and noncommon (XOR operation) area of two contours with to the total area (OR operation).

The summary of assessment for ten images is listed in Table 3. Three degrees – Good, Fair, and Bad are used to classify the assessment results. When l_{AND} is in the scope of 0.900 ~ 1.000, the result is marked good. When l_{AND} in 0.750~0.900, the result is Fair. And when l_{AND} in 0 ~ 0.750, the result is bad. Fig. 8 and Fig. 9 show two results that compare the expert's delineation and automatic detection.

Table 3: Assessment of the detection results for innermost boundary and outer boundary of the third layer on rectal image

Image number	Tumor boundary			Image number	Tumor boundary		
	Relative similarity l_{AND}	Relative difference l_{XOR}	Evaluation		Relative similarity l_{AND}	Relative difference l_{XOR}	Evaluation
1	0.8637	0.1363	Fair	6	0.9144	0.0856	Good
2	0.8188	0.1083	Fair	7	0.7765	0.2235	Fair
3	0.9300	0.0700	Good	8	0.7911	0.2089	Fair
4	0.8854	0.1146	Fair				
5	0.8813	0.1169	Fair				

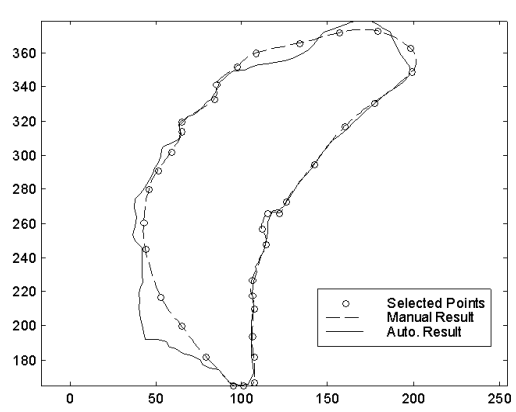

(a) Automatic detecting result and manually delineating result (b) XOR result (white region) of two areas

Fig. 8: Comparison of automatic results with manual results (Image no. 19991025_06.bmp) (Note: The image coordinates are different from Cartesian coordinate. The origin of the image coordinate is at top left corner).

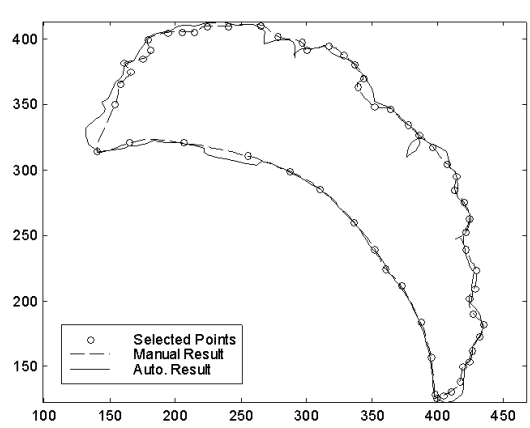

(a) Automatic detecting result and manually delineating result (b) XOR result (white region) of two areas

Fig. 9: Comparison of automatic results with manual results (Image no. 19991101_2.bmp).

4. CONCLUSION

We proposed a novel active contour model unifying the region-based and gradient-based features from the image. The new active contour model is set up under three energy modules: internal energy of the contour, region energy of the image and gradient energy of the image. As a result, the deformation of the active contour is driven under the corresponding kinetic function derived from its energy function. The region-based image feature represents the statistical information from the seed region of the contour. Here, a Gaussian Mixture Model is proposed to accurately describe the region statistical features. Expectation-Maximization algorithm is used for optimal parameter estimation for this GMM.

The experimental results demonstrate the addition of region-based feature gives more flexibility for the active contour model than traditional snake algorithm and accelerates the velocity of the convergence. It doesn't need the initial contour to be placed at the gradient capture range of the desired boundary as snake method. It more emphasizes the region information from the initial active contour. The procedure of boundary finding is a combined effect of the

internal force, region force and gradient force. One of the important things in our algorithm is the construction of Gaussian Mixture Model and its parameter estimation by EM algorithm ensures the accurate statistical description for seed region. The experimental results also show it is suitable for tumor boundary detection on a rectal wall ultrasound image.

Some shortcomings are also existed with this unifying active contour model. If the initial active contour is placed on a wrong region, the incorrect statistical feature will be obtained and will influence the performance of the active contour. The sensitivity from weighting coefficients is also existed like that in snake algorithm.

REFERENCES

1. J. F. Haddon, & J. F. Boyce, "Image Segmentation by Unifying Region and Boundary Information", *IEEE Transactions on Pattern Analysis and Machine Intelligence*, **12**, pp. 929-948, 1990.
2. T. Pavlidis, & Y.-T. Liow, "Integrating region growing and edge detection", *IEEE Transactions on Pattern Analysis and Machine Intelligence*, **12**, pp. 225–233, 1990.
3. T. Pavlidis, & Y.-T. Liow, "Integrating region growing and edge detection. Computer Vision and Pattern Recognition", *Proceedings CVPR '88.*, pp. 208–214, 1988.
4. J.-H. Xuan, & T. Adali, &Y. Wang, "Segmentation of magnetic resonance brain image: integrating region growing and edge detection", *International Conference on Image Processing*, **3**, pp. 544–547, 1995.
5. T. F. Chan, & L. A. Vese, "A level set algorithm for minimizing the Mumford-Shah functional in image processing", *IEEE Workshop on Variational and Level Set Methods in Computer Vision*, pp. 161–168, 2001.
6. T. F. Chan, & L. A. Vese , "Active Contours Without Edges", *IEEE Trans. on Image Processing*, **10**, pp. 266-277, 2001.
7. Song Chun Zhu, & Alan Yuille, "Region Competition: Unifying Snakes, Region Growing, and Bayes/MDL for Multiband Image Segmentation", *IEEE Transactions on Pattern Analysis and Machine Intelligence*, **18**, pp. 884-900, 1996.
8. A.P. Pentland, "Automatic Extraction of Deformable Part Models", *International Journal of Computer Vision*, **4**, pp. 107-126, 1990.
9. A. Leonardis, & A. Gupta, & R. Bajcsy, "Segmentation of Range Images as the Search for Geometric Parametric Models", *International Journal of Computer Vision*, **14**, pp. 253-277, 1995.
10. A. Chakraborty, & L. H. Staib, & J. S. Duncan, "Deformable Boundary Finding in Medical Images by Integration Gradient and Region Information" *IEEE Transactions on Medical Imaging*, **15**, pp. 859-870, 1996.
11. N. Paragios, & R. Deriche, "Unifying boundary and region-based information for geodesic active tracking", *IEEE Computer Society Conference on Computer Vision and Pattern Recognition*, **2**, pp. 300-305, 1999.
12. N. Paragios, & R. Deriche, "Geodesic active regions for supervised texture segmentation", *The Proceedings of the Seventh IEEE International Conference on Computer Vision*, **2**, pp. 926–932, 1999.
13. N. Paragios, & R. Deriche, "A variational approach for the segmentation of the left ventricle in MR cardiac images", *IEEE Workshop on Variational and Level Set Methods in Computer Vision*, pp. 153–160, 2001.